Journal of Applied Mechanics and Technical Physics, Vol. 42, No. 2, pp. 202–210, 2001

DAMPING PROPERTIES OF SEQUOIA, BIRCH, PINE, AND ASPEN UNDER SHOCK LOADING

A. P. Bol'shakov,[1] M. A. Balakshina,[1] N. N. Gerdyukov,[1] E. V. Zotov,[1] A. K. Muzyrya,[2] A. F. Plotnikov,[2] S. A. Novikov,[1] V. A. Sinitsyn,[1] D. I. Shestakov,[2] and Yu. I. Shcherbak[1]

UDC 674.038.1

Results of an experimental study of strength–deformation properties of sequoia, aspen, pine, and birch wood for various loading rates, temperatures, humidities, and orientation angles of wood fibers with respect to the loading direction are described. Stress–strain diagrams and an analytical dependence of strength on humidity, temperature, and loading rate are presented.

A widely distributed natural material, wood, has recently gained, due to its specific properties (relatively low density, relatively high mechanical strength, low heat conductivity, and technological effectiveness), extensive application not only in civil engineering but also in some other fields of technology. The property to deform, under lateral compression, in a wide range of strains (30–40%) with a practically constant stress categorizes wood as a material capable of damping shocks [1–4]. As a shock absorber, wood restricts the transmitted load at a level of its ultimate strength. In conjunction with a relatively low cost and simplicity of technological operations required for wood processing, the latter makes it possible to use the material as a limiter of accidental shocks (damper) in transportation of goods whose destruction during accidents may lead to severe ecological hazards. In designing protection systems employing wood dampers, data are required on strength-deformation properties of particular types of wood.

In the present paper, some results of static and dynamic uniaxial testing of wood samples of four types (birch, sequoia, pine, and aspen) are described.

Most samples in this study were prepared according to Russian national standards. The difference in linear dimensions (lengths of longitudinal or transverse ribs) of prismatic samples was within 0.1 mm. The same is also valid for heights and diameters of cylindrical samples. The right angles between the adjacent faces were controlled using a try square. The roughness of the working surfaces of the samples complied with the requirements specified in the standard GOST 16 483.0-89 ("Wood. General requirements to physical-mechanical testing procedures") was within 100 μm and was controlled with a watch-type indicator.

1. STRENGTH AND DEFORMATION PROPERTIES OF SEQUOIA AND BIRCH

Experimental Conditions and Instrumentation. Strength and deformation properties of sequoia wood (U.S.A) and birch wood (Volga–Vyatka Region, Russia) under dynamic (10 m/sec) and quasistatic (approximately 10^{-4} m/sec) loading rates were studied. Previously, extensive data on the strength and deformation properties of birch were reported in [5, 6]. In the present paper, some data for birch are given for

[1]Institute of Experimental Physics, Sarov 607190. [2]Institute of Technical Physics, Snezhinsk 456770.
Translated from Prikladnaya Mekhanika i Tekhnicheskaya Fizika, Vol. 42, No. 2, pp. 23–32, March–April, 2001. Original article submitted November 18, 1999; revision submitted April 12, 2000.

0021-8944/01/4202-0202 $25.00

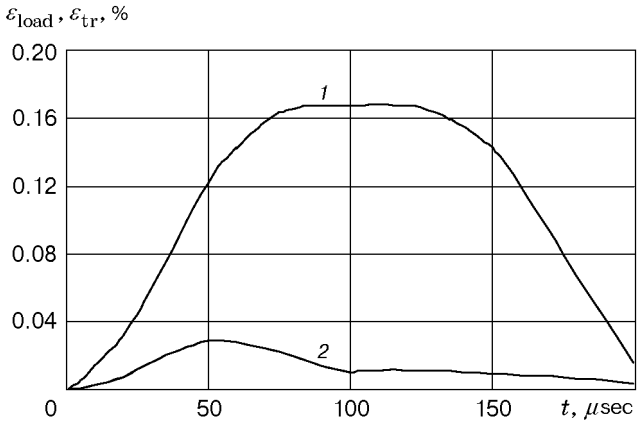

Fig. 1. Elastic strain versus time in loading stress wave (curve 1) and traveling stress wave (curve 2) for birch at $\alpha = 10^\circ$ and $T = 20^\circ$C.

comparison with other types of wood. Cylindrical samples of identical (25 mm) heights and diameters cut at angles of 0, 5, 10, 15, 30, 45, and 90° to the wood-fiber direction were put to a test for uniaxial compression at temperatures of −30, 20, and 65°C; their humidity $\omega = 6$–7% being fixed. Dynamic tests were conducted according to the Kolski method on a setup with a composite Hopkinson rod [7, 8]. The loading procedure based on using an explosive device and the measurement scheme were described in [5, 6]. Heating and cooling of the samples were performed in special thermostats. Liquid nitrogen was used as a coolant. To avoid moisture losses, the samples were packed in sealed 0.02 mm-thick polyethylene packets, in which they were subsequently tested. The samples were loaded with trapezoidal pressure pulses with a 0.2-MPa amplitude and a 200-μsec duration. All tests were conducted under laboratory conditions.

Experimental Results. In each test, resistance strain gages fixed to measuring rods (loading and reference ones) measured the value of elastic strains in loading stress wave ($\varepsilon_{\text{load}}$) and the value of elastic strains in traveling stress wave (ε_{tr}) (Fig. 1). From the experimentally measured strains $\varepsilon_{\text{load}}(t)$ and $\varepsilon_{\text{tr}}(t)$, the averaged values of the uniaxial-compression stress σ_s and strain ε_s in the direction of wave propagation in the sample were determined from the following formulas [8]:

$$\sigma_s(t) = \frac{\varepsilon_{\text{tr}}(t) E F_{\text{rod}}}{F_{\text{sample}}}, \qquad \varepsilon_s(t) = \frac{2a}{l} \int_0^t [\varepsilon_{\text{load}}(t) - \varepsilon_{\text{tr}}(t)]\, dt.$$

Here E is the elasticity modulus of the rod material, F_{rod} and F_{sample} are the cross-sectional areas of the rod and sample, respectively, a is the propagation velocity of elastic waves in the rod, and l is the sample length. The experimental errors in determination of both stress and strain were within ±10%.

The sample-loading rate v was determined from the highest stress $\sigma_{\max}$ in the loading compression wave using the formula $v = \sigma_{\max}/(\rho a)$, where ρ is the density of the rod material.

By precise control over the mass of a liquid explosive in the loading setup, the highest load $\sigma_{\max}$ in the experiments was maintained at a constant level (about 225 ± 5 MPa). The latter ensured a constant loading rate v of 10 m/sec. The tests were conducted under quasistatic loading with a loading rate v of 10^{-4} m/sec on an R-5 rupture machine. A desired temperature was ensured by thermostats.

The dynamic σ–ε diagrams of sequoia wood with wood fibers oriented at angles α ranged from 0 to 90° with respect to the loading direction are shown in Fig. 2 (for a temperature of −30°C). The dynamic diagrams of sequoia- and birch-wood deformation at temperatures of 20 and 65°C, as well as quasistatic diagrams, display a similar domelike shape (except for diagrams obtained for $\alpha = 90^\circ$). The main difference between the dynamic and quasistatic diagrams is a lower (by a factor of 1.5–2) failure strain ε_* (under the highest compression stress σ_*). A considerable decrease in the stress peak (from several percent to 6–8 times) observed as the fiber angle increases from 0 to 45° is a characteristic feature displayed by all σ–ε diagrams. Under lateral compression ($\alpha = 90^\circ$), the deformation of the two types of wood proceeds at a nearly constant

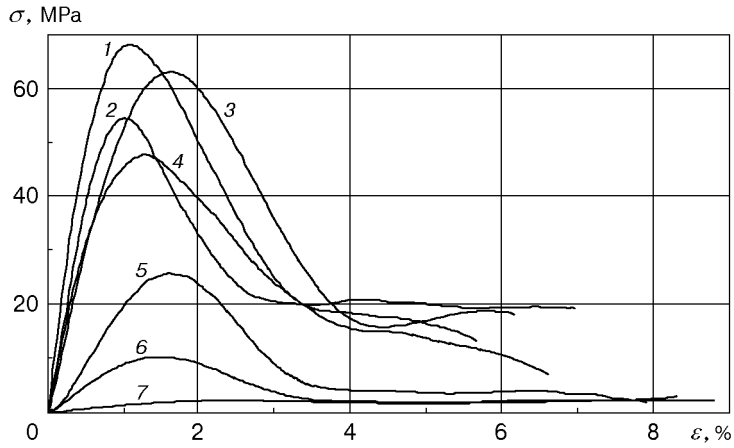

Fig. 2. Dynamic σ–ε diagrams of sequoia wood for $T = -30°$C and $\alpha = 0$ (1), 5° (2), 10° (3), 15° (4), 30° (5), 45° (6), and 90° (7).

TABLE 1

Dynamic and Static Strengths of Sequoia and Birch Samples As Functions of the Fiber Angle and Temperature

α, deg	ρ, kg/m^3	σ_*, MPa						ε_*, %					
		−30°C		20°C		65°C		−30°C		20°C		65°C	
		dyn.	stat.	dyn.	stat.	dyn.	stat.	dyn.	stat.	dyn.	stat.	dyn.	stat.
		Sequoia											
0	418	68.0	51	40.2	48	55.3	56	1.1	2.6	1.4	3.3	1.4	3.3
5	405	54.5	53	37.1	50	47.4	49	1.0	2.4	1.2	2.7	1.4	3.2
10	408	63.0	43	43.3	48	48.7	45	1.6	2.0	1.6	3.0	1.2	2.9
15	417	47.7	40	45.3	36	27.0	38	1.3	2.0	1.6	1.6	0.5	1.8
30	412	25.7	16	26.8	21	17.7	18	1.6	1.7	1.0	1.7	1.1	2.2
45	370	10.1	8	11.4	9	13.1	8	1.4	2.2	1.4	2.2	0.6	1.0
90	420	2.0	3.8	4.0	3.7	3.0	3.7	—	33.0	—	36.0	—	31.0
		Birch											
0	624	128	88	105	81	104	86	1.5	2.7	1.3	2.1	1.6	2.4
5	600	119	85	108	81	94	78	1.1	1.4	1.4	1.6	1.8	1.9
10	603	57	65	77	65	61	58	1.1	1.7	1.1	2.8	1.6	2.9
15	627	65	71	81	66	68	74	1.5	1.6	1.4	3.4	1.2	2.0
30	633	34	38	35	35	32	35	1.5	3.3	1.7	4.2	1.5	3.6
45	609	17	24	19	23	18	16	2.6	2.8	2.0	4.6	1.7	2.7
90	590	8	12	12	11	10	10	—	32.0	—	41.0	—	38.0

stress (2–4 MPa for sequoia and 8–12 MPa for birch) up to $\varepsilon = 30$–40% (under quasistatic loading). As wood is further compressed, wood layers become more consolidated and stress increases. For dynamic lateral compression, the σ–ε diagrams were plotted up to strains of 10–12%. A typical feature of failure of sequoia and birch samples with $\alpha = 0$, 5, 10, and 15° is the formation of cracks observed on attaining the stress peak (failure stress σ_*) and their further development throughout the whole sample observed with decreasing stress. Further deformation of the samples results in longitudinal splitting and wood-fiber fracture. For failure of the samples with $\alpha = 30$ and 45°, cleavage at the same angles is typical. The failure of birch and sequoia samples with fiber angles ranging from 0 to 45° starts at $\varepsilon = 1$–3%. Under lateral compression to about 50%, wood layers experience compaction without failure.

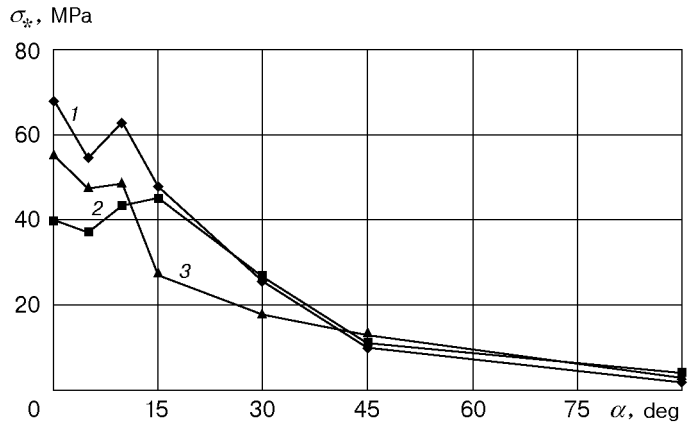

Fig. 3. Dynamic strength σ_* of sequoia versus the fiber angle α for $T = -30$ (1), 20 (2), and 65°C.

The data on sequoia and birch are listed in Table 1. The dependences of the ultimate strength σ_* of sequoia on the fiber angles $\alpha = 0$, 5, 10, 15, 30, 45, and 90° for $T = -30$, 20, and 65°C are shown in Fig. 3.

The values of practically constant lateral-compression stresses for the wood samples tested are one order of magnitude lower than longitudinal-compression failure stresses. The mechanical strength of sequoia wood with a 6–7% humidity is almost independent of temperature and loading rate. An appreciable increase in the sequoia-wood strength is observed only for a loading rate of 10 m/sec and a temperature of −30°C. The tests of birch-wood samples with fiber angles $\alpha = 0$ and 5° performed at $T = -30$, 20, and 65°C revealed a higher dynamic strength than tests with other fiber angles. For the above-indicated temperatures and fiber angles, the dynamic-strength coefficients of birch wood were 1.4, 1.3, and 1.2, respectively. It also follows from the data obtained that the mechanical strength of birch samples with fiber angles $\alpha = 0$ and 5° decreases substantially as the temperature increases. For instance, under dynamic loading with increasing temperatures ($T = -30$, 20, and 65°C), the mechanical strength of birch samples decreases from 128 to 104 MPa for $\alpha = 0$ and from 119 to 94 MPa for $\alpha = 5°$. Under quasistatic loading, other conditions being equal, the mechanical strength of birch wood decreases with increasing temperature from 88 to 81 MPa and from 85 to 78 MPa. Comparing the compression strength σ_* of birch wood with that of sequoia, one can easily find that the sequoia strength is 1.5–2 times as low as the birch strength for all fiber angles.

2. STRENGTH AND DEFORMATION PROPERTIES OF PINE AND ASPEN

Test Conditions and Instrumentation. Up to date, no data were reported on the mechanical behavior of pine and aspen wood for various loading rates and negative temperatures [9–14]. This paper presents some experimental data on the stress–strain characteristics of pine and aspen wood obtained under the following conditions:

— loading rates of about $2 \cdot 10^{-5}$ m/sec (quasistatic loading) and 7 and 13 m/sec (dynamic loading);
— three levels of wood humidity (5, 20, and more than 30%);
— three temperatures (−40, 20, and 50°C);
— deformation along wood fibers in the radial and tangential directions.

Pine and aspen wood samples for compression tests had standard sizes (20 × 20 × 30 mm). They were cut in three different directions with respect to the fibers (longitudinal, radial, and tangential ones). The humidity of the samples was determined as the difference between the sample masses prior to and after drying. (According to the accepted standard, the humidity is defined as the ratio of the mass of water in the sample to the mass of absolutely dry wood. For the so-called wet wood, the humidity may be greater than 100%.) The desired test temperatures of 20 and 50°C were obtained by placing the samples into a

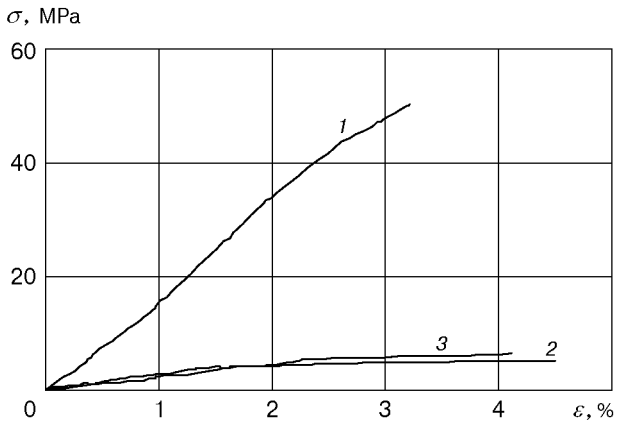

Fig. 4. Static σ–ε diagrams of pine wood for different compression directions with respect to wood fibers ($T = 20°$C and $\omega = 4\%$): 1) tangential; 2) along wood fibers; 3) radial.

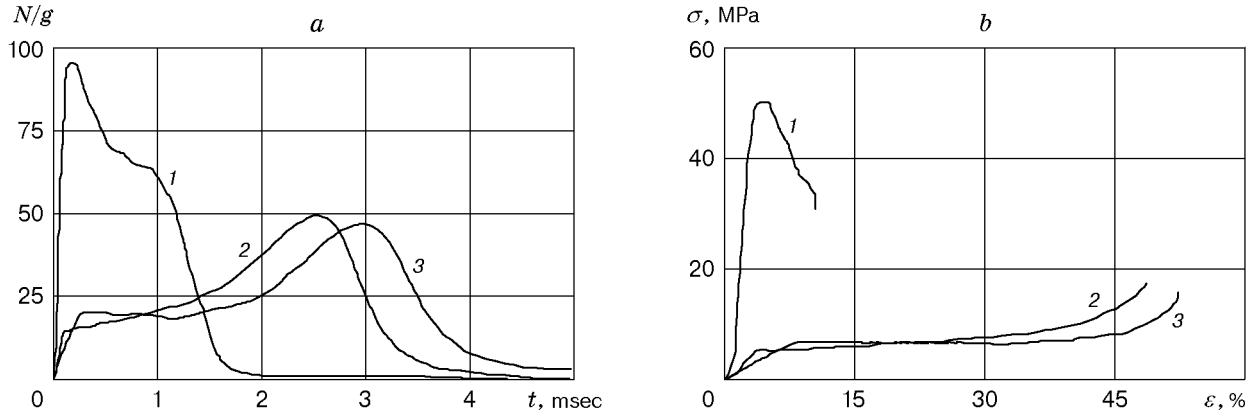

Fig. 5. Experimental dependences of the overload $N(t)$ (a) and the calculation diagrams $\sigma(\varepsilon)$ (b) for different compression directions of pine wood ($T = 20°$C, $\omega = 18$–20%, and $V = 6.7$–6.8 m/sec): 1) along fibers; 2) radial; 3) tangential.

constant-temperature cabinet and keeping them there during 1 h. To avoid losses of moisture, the samples were packed in sealed polyethylene packets. The temperature of $-40°$C was ensured by placing the samples into a thermostat. Liquid nitrogen was used as a coolant.

Quasi-static mechanical properties of the samples under compression were determined on a universal test apparatus "Instron-1185" (England) equipped with a climate chamber. The stress–strain diagrams were recorded for a strain rate of 1 mm/min. The error in load measurements was $\pm 1\%$, and that in strain measurements was 3–8%. The mean values of mechanical characteristics of the samples were found from test data obtained for 4–10 samples.

Dynamic tests were carried out on a shock table, which had the following characteristics: impact velocity up to 13 m/sec and mass of the falling hammer 2.37 kg. The impact velocity V was determined with the help of electric contacts from the measured period during which the hammer traversed a certain distance. The impact force was determined from hammer overloads $N(t)$ measured with the help of piezoaccelerometers. The measurement error was $\pm(6$–$13)\%$. The strain evolution in time was determined by integration of the measured dependence $N(t)$. By the first integration, we determined the displacement velocity of the hammer–sample interface and, by the second integration, the spatial location of the interface, i.e., sample contraction and, hence, strain. Special tests were performed to test the procedure itself, with immediate measurements of strains with the help of electric contacts. In dynamic tests, experimental statistics was determined from measurement data for three samples tested under identical conditions.

TABLE 2

Compression Strength and Deformation Characteristics of Pine Wood for Different Humidities, Temperatures, and Loading Rates

Compression direction	T, °C	Dry wood ($\omega < 6\%$)					Moist wood ($\omega = 18$–20%)					Wet wood ($\omega > 30\%$)				
		V, m/sec	ω, %	ρ, kg/m^3	σ, MPa	ε, %	V, m/sec	ω, %	ρ, kg/m^3	σ, MPa	ε, %	V, m/sec	ω, %	ρ, kg/m^3	σ, MPa	ε, %
Along wood fibers	20	0	3.9	420	57.9	3.1	0	20	460	24.5	4.7	0	68	570	20.2	4.2
		6.8	3.9	400	69.0	4.5	6.7	18	460	47.4	3.7	6.7	68	600	41.6	3.9
		11.7	3.9	400	78.4	7.5	12.2	19	480	66.8	3.5	12.4	133	800	38.8	2.1
	−40	0	4.1	430	85.0	1.4	0	18	470	64.3	1.6	0	136	800	55.0	12.2
		5.7	4.1	500	124.6	2.9	6.7	18	470	77.2	3.2	6.7	133	800	56.0	2.5
		12.0	4.1	500	125.4	4.2	12.2	18	470	120.4	4.7	12.3	136	800	77.3	4.5
	50	0	4.1	450	62.5	1.3	0	18	460	31.4	1.3	0	136	810	17.0	2.3
		5.8	4.1	440	79.9	4.2	6.7	18	490	54.5	1.8	6.0	136	800	28.2	3.2
		11.9	4.1	430	103.7	4.0	12.2	18	480	43.5	4.3	11.9	136	800	32.4	2.3
Radial	20	0	3.9	425	3.8	1.1 (−)	0	20	480	2.9	1.6 (−)	0	68	610	1.9	1.0 (−)
		6.8	3.9	400	7.0	3.5 (34)	6.7	18	470	5.4	3.6 (32)	6.7	68	560	4.0	5.0 (27)
		11.7	4.0	400	5.1	5.3 (41)	12.4	19	490	4.1	2.9 (34)	12.4	133	800	3.5	3.0 (−)
	−40	0	4.1	490	4.8	1.3 (−)	0	18	480	3.8	1.8 (−)	0	136	860	11.1	2.1 (−)
		5.7	4.1	460	8.7	42 (32)	6.8	18	460	6.5	5.0 (35)	6.7	133	800	26.0	9.0 (−)
		12.0	4.1	470	6.7	3.8 (45)	12.3	18	460	7.3	5.8 (38)	12.3	136	870	29.6	8.6 (−)
	50	0	4.1	460	3.2	0.8 (−)	0	18	470	2.4	2.3 (−)	0	136	820	1.4	1.8 (−)
		5.8	4.1	440	6.0	3.7 (31)	6.9	19	480	4.6	2.4 (31)	6.0	136	860	3.6	6.3 (−)
		11.9	4.1	430	5.5	4.3 (40)	12.6	19	470	4.1	3.0 (38)	11.9	136	850	3.3	4.2 (−)
Tangential	20	0	3.9	425	5.5	2.2 (−)	0	20	480	3.1	4.2 (−)	0	68	620	2.0	1.6 (−)
		6.8	3.9	390	7.0	4.3 (52)	6.8	20	450	6.5	7.8 (43)	6.7	68	630	5.8	5.3 (33)
		11.7	3.9	410	8.2	9.7 (48)	12.6	19	480	7.0	4.5 (51)	12.4	133	800	5.8	7.7 (50)
	−40	0	4.1	410	6.8	2.1 (−)	0	18	480	7.0	2.0 (−)	0	136	850	12.0	2.4 (−)
		5.7	4.1	470	15.7	3.0 (−)	6.8	18	480	14.0	6.0 (−)	6.7	133	770	13.0	9.0 (−)
		12.0	4.1	470	12.5	4.0 (−)	12.3	18	460	13.0	6.5 (−)	12.3	136	830	33.0	8.0 (−)
	50	0	4.1	470	6.2	2.4 (−)	0	18	470	3.3	3.3 (−)	0	136	800	1.6	1.6 (−)
		5.8	4.1	440	6.9	3.6 (40)	6.9	18	480	6.7	4.0 (47)	6.9	136	780	3.5	2.0 (50)
		11.9	4.1	430	6.9	3.5 (53)	12.6	18	480	6.8	4.0 (52)	11.9	136	780	3.9	3.8 (63)

Note. The largest strains at which the damping properties are still retained are given in brackets.

TABLE 3

Compression Strength and Deformation Characteristics of Aspen Wood for Different Humidities, Temperatures, and Loading Rates

Compression direction	T, °C	Dry wood ($\omega < 6\%$)					Moist wood ($\omega = 18$–20%)					Wet wood ($\omega > 30\%$)				
		V, m/sec	ω, %	ρ, kg/m^3	σ, MPa	ε, %	V, m/sec	ω, %	ρ, kg/m^3	σ, MPa	ε, %	V, m/sec	ω, %	ρ, kg/m^3	σ, MPa	ε, %
Along wood fibers	20	0	4.8	450	60.5	1.5	0	29	520	20.0	2.9	0	85	730	22.8	2.1
		7.0	4.8	440	90.1	3.3	7.0	18	560	37.0	2.3	6.9	59	660	35.8	2.0
		12.5	4.8	440	112.0	3.9	12.8	18	440	50.1	4.3	12.6	85	750	35.3	4.0
	−40	0	4.8	450	93.0	2.2	0	29	460	43.5	2.8	0	85	740	51.0	1.8
		7.0	4.8	440	73.6	4.6	7.0	18	540	89.5	3.4	6.9	59	640	73.6	3.1
		12.5	4.8	440	104.0	4.0	12.8	18	510	93.3	4.1	12.6	85	750	86.5	4.6
	50	0	5.4	440	45.5	1.6	0	26	550	22.0	2.2	0	59	660	17.9	2.7
		7.0	5.4	450	69.8	2.7	7.0	18	550	38.8	2.7	6.9	59	650	32.5	1.8
		11.9	5.4	440	74.5	6.2	12.8	18	530	36.6	4.0	12.6	85	750	27.6	8.0
Radial	20	0	4.8	450	5.4	2.2 (−)	0	29	550	1.4	3.0 (−)	0	85	710	1.6	2.2 (−)
		7.0	4.8	440	10.1	4.3 (38)	7.0	18	560	5.4	3.9 (31)	6.9	59	680	4.0	2.1 (30)
		12.5	4.8	440	8.7	5.5 (45)	12.9	18	440	4.7	4.7 (35)	12.6	85	750	3.8	4.0 (29)
	−40	0	4.8	450	8.1	2.1 (−)	0	29	480	2.9	3.7 (−)	0	85	760	5.7	2.0 (−)
		7.0	4.8	430	7.8	4.0 (27)	7.0	18	560	10.0	2.1 (−)	6.9	59	630	11.2	4.0 (−)
		12.5	4.8	440	8.4	6.2 (58)	12.8	18	460	8.3	6.6 (49)	12.6	85	760	15.7	7.3 (−)
	50	0	5.4	430	4.4	1.5 (−)	0	26	550	2.5	2.6 (−)	0	59	670	1.4	3.2 (−)
		7.0	5.4	460	7.0	5.0 (−)	7.0	18	580	4.6	3.3 (28)	6.9	59	650	3.2	2.2 (26)
		11.9	5.4	430	6.6	4.4 (46)	12.8	18	520	2.8	5.4 (39)	12.6	85	740	3.2	4.9 (26)
Tangential	20	0	4.8	450	4.1	1.9 (−)	0	29	530	1.9	2.5 (−)	0	85	730	1.9	2.2 (−)
		7.0	4.8	430	7.4	5.5 (29)	7.0	18	550	4.4	4.9 (24)	6.9	59	680	3.8	4.8 (29)
		12.5	4.8	450	6.8	7.3 (33)	12.8	18	470	5.8	6.4 (39)	12.6	85	750	4.2	4.5 (35)
	−40	0	4.8	450	6.0	2.0 (−)	0	29	470	3.8	2.4 (−)	0	85	740	8.4	2.4 (−)
		7.0	4.8	420	7.0	7.1 (31)	7.0	18	570	9.3	5.1 (24)	6.9	59	660	14.7	7.3 (−)
		12.5	4.8	440	7.0	5.3 (64)	12.8	18	440	9.3	5.9 (51)	12.6	85	750	21.5	12.5 (−)
	50	0	5.4	440	3.8	2.7 (−)	0	26	550	1.8	4.7 (−)	0	59	660	1.3	2.2 (−)
		7.0	5.4	460	6.5	7.8 (34)	7.0	18	560	3.4	3.1 (26)	6.9	59	650	3.2	1.6 (24)
		11.9	5.4	450	6.1	7.4 (32)	12.8	18	520	3.6	3.8 (37)	12.6	85	740	3.3	4.3 (33)

Note. The largest strains at which damping properties are still retained are given in brackets.

TABLE 4

Constants Entering Analytical Dependence (1)

Compression direction	σ_ω, MPa		σ_0, MPa		k_1, MPa/°C		k_2, MPa · sec/m	
	pine	aspen	pine	aspen	pine	aspen	pine	aspen
Along fibers	30.0	33.0	80.0	77.0	0.350	0.400	2.10	2.00
Radial	3.0	2.2	5.0	7.3	0.020	0.020	0.16	0.20
Tangential	4.4	2.9	8.0	2.7	0.055	0.026	0.28	0.22

Experimental Results. Typical stress–strain diagrams obtained in static tests and also acceleration curves for dynamic loading are shown in Figs. 4 and 5. Some data extracted from these diagrams are tabulated in Tables 2 and 3.

The major part of the results obtained can be approximately described by the following trinomial relation:

$$\sigma(\omega, T, V) = \sigma_\omega + (\sigma_0 - \sigma_\omega) \exp\left[-(\omega/C)^2\right] - k_1 T + k_2 V. \tag{1}$$

Here ω is the humidity of wood, σ_ω is the mechanical strength for $\omega > 30\%$, $T = 0$, $V = 0$, σ_0 is the mechanical strength of absolutely dry wood ($\omega = 0$, $T = 0$, and $V = 0$), C is an empirical coefficient, and k_1 and k_2 are the temperature and velocity coefficients, respectively. We chose this relation based on the exponential dependence of the mechanical strength on humidity and the linear dependence on temperature proposed in [15]. Here, we took into account a linear increase in mechanical strength proportional to impact velocity. The numerical values of the constants in Eq. (1) are listed in Table 4. We had $C = 16\%$ in all experiments with pine and aspen samples and for all fiber angles.

For the radial and tangential directions of deformation, dependence (1) fails to describe a specific region, that of negative sample temperatures and humidity over 30%. In this region, because of freezing, the material acquires an enhanced mechanical rigidity. A frozen specimen of wet wood offers significant resistance to radial and tangential deformation. The growth rate of the mechanical load and the mechanical strength in this case are greater than in tests at positive temperatures and comparable with the rate and strength displayed under loading the sample in the "strongest" direction (along the wood fibers). The latter results in an abrupt change in the mechanical strength of wood at −40°C (for $\omega > 30\%$).

Thus, it is shown that the anisotropy of pine and aspen samples leads to anisotropy of their strength characteristics under quasistatic and dynamic loadings.

Under compression in the radial and tangential directions, a typical picture of elastoplastic deformation followed by rigid unloading is observed.

For the ranges of humidity (from 0 to 130%), temperature (from −40 to 50°C), and impact velocity (from $2 \cdot 10^{-5}$ to 13 m/sec) studied in this work, the experiments performed allow the following conclusions to be made:

— The mechanical strengths of pine and aspen wood decrease as the humidity increases to 30% and attain a plateau with further increase in humidity;

— The pine and aspen mechanical strengths decrease as the temperature rises;

— The mechanical strengths of pine and aspen increase on passing from static to dynamic loading.

For extreme values of the parameters involved, the behavior of a sample loaded in the radial or tangential directions changes. For a humidity above 30% and a temperature of −40°C, the frozen sample offers strong resistance to an impact, similarly to the case of loading along the fibers.

The experimental data for pine and aspen wood can be described within ±25% by a simple trinomial relation (1), which takes into account the dependence of mechanical strength on humidity (exponential decrease), temperature (linear decrease), and impact velocity (linear increase).

The authors thank S. V. Sen'kova for her kind assistance in processing experimental data and preparing documentation.

This work was performed under Contract Nos. AJ-286 and AJ-3224 with Sandia National Laboratories (Albuquerque, U.S.A.). This work was also supported by the Russian Foundation for Fundamental Research (Grant No. 97-01-00344).

REFERENCES

1. Yu. A. Krysanov and S. A. Novikov, "Dynamic-compression study of expanded polystyrene," *Probl. Prochn.*, No. 8, 115–117 (1977).
2. S. A. Novikov, V. A. Sinitsyn, and A. P. Pogorelov, "Designing an explosive loading device for generation of pressure pulses with preset parameters," *Fiz. Goreniya Vzryva*, **16**, No. 6, 111–113 (1980).
3. A. I. Abakumov, G. A. Kvaskov, S. A. Novikov, and V. A. Sinitsyn, "Study of elastoplastic deformation of cylindrical shells with axial shock loading," *Prikl. Mekh. Tekh. Fiz.*, **29**, No. 3, 150–153 (1988).
4. B. V. Bagryanov, G. A. Kvaskov, S. A. Novikov, and V. A. Sinitsyn, "Axial dynamic compression of tubular metal crushers," *Prikl. Mekh. Tekh. Fiz.*, **23**, No. 1, 156–159 (1982).
5. A. P. Bol'shakov, N. N. Gerdyukov, E. V. Zotov, et al., "Effect of the loading rate, angle of orientation of fibers, and temperature on the strength properties of birch," *Prikl. Mekh. Tekh. Fiz.*, **39**, No. 6, 154–158 (1998).
6. A. P. Bol'shakov, N. N. Gerdyukov, E. V. Zotov, et al. "Damping properties of redwood and birch at shock loading," in: *Proc. of the 12th Int. Conf. on the Packaging and Transportation of Radioactive Materials* (Paris, May 10–15, 1998), Vol. 1, Palais des Congres, Paris (1998), pp. 269–274.
7. A. P. Bol'shakov, S. A. Novikov, and V. A. Sinitsyn, "Strength of construction materials under dynamic loads (an overview)," in: *Questions of Atomic Science and Engineering*, Ser. *Physics and Technology of Nuclear Reactors*, No. 1, (1989), pp. 23–46.
8. J. A. Zykas, et al., *Impact Dynamics*, Wiley, New York (1982).
9. A. M. Borovikov and B. N. Ugolev, *Handbook on Wood* [in Russian], Lesn. Promyshl., Moscow (1989).
10. É. A. Satel' (ed.), *Mechanical Engineer's Handbook* [in Russian], Vol. 6, Mashinostroenie, Moscow (1964).
11. V. E. Moskaleva, *Wood Structure and Its Changes Under Physical and Mechanical Factors* [in Russian], Izd. Akad. Nauk SSSR, Moscow (1957).
12. N. L. Leont'ev, "Study of physicomechanical properties of Kol'skaya pine wood," in: *Physicomechanical Properties of Wood* (collected scientific papers) [in Russian], Goslesbumizdat, Moscow–Leningrad (1953).
13. G. I. Pogodin-Alekseev (ed.), *Handbook on Macnine-Building Materials* [in Russian], Vol. 4, Mashgiz, Moscow (1960).
14. B. N. Ugolev, *Testing of Wood and Wood Materials* [in Russian], Lesn. Promyshl., Moscow (1965).
15. V. N. Volynskii, "Effect of humidity and temperature on mechanical characteristics of wood with allowance for its density," *Izv. Vyssh. Ucheb. Zaved., Lesn. Zh.*, No. 5, 75–79 (1991).